

Fig. 7. Oscillation power level as a function of phase  $\theta$  of load at  $|\Gamma|=1$ , 8.2 GHz.

confirmed by the experiment. The tuning frequency range of the experimental oscillator is restricted by the characteristics of the 3-dB directional coupler being used, so a tunable frequency range of the oscillator with the circuit

can be made wider by utilizing a wider frequency band 3-dB directional coupler. The proposed YIG resonator circuit will be naturally applicable to other negative resistance type oscillators like that of an IMPATT diode oscillator, but for the application to the more high power oscillator, some careful considerations about the nonlinear effect of YIG sample will be required.

#### ACKNOWLEDGMENT

The authors would like to acknowledge the great technical assistance of M. Washio of the Academy and that of S. Tamura.

#### REFERENCES

- [1] F. Okada, K. Ohwi, and S. Tamura, 1977 Conv. Rec. IECE of Japan, no. 579, Mar. 1977.
- [2] R. E. Tohkeim, C. K. Greene, J. C. Hoover, and R. W. Peter, "Nonreciprocal YIG filters," *IEEE Trans. Magn.*, vol. MAG-3, pp. 383-392, Sept. 1967.
- [3] M. Igarashi and Y. Naito, "Properties of a four-port nonreciprocal circuit utilizing YIG on stripline—Filter and circulator," *IEEE Trans. Microwave Theory Tech.*, vol. MTT-20, pp. 828-833, Dec. 1972.
- [4] B. Lax and K. J. Button, *Microwave Ferrite and Ferrimagnetics*. McGraw-Hill, 1962.
- [5] F. Okada and K. Ohwi, *IECE of Japan, Trans.*, vol. 58-B, no. 4, p. 156, Apr. 1975.

## Reflection of Magnetostatic Forward Volume Waves by a Shallow-Grooved Grating on a YIG Film

JAYANTKUMAR P. PAREKH, MEMBER, IEEE, AND HANG-SHENG TUAN, MEMBER, IEEE

**Abstract**—The magnetostatic forward volume wave (MSFVW) reflection characteristics of a uniform grating of shallow grooves etched on the planar surface of an epitaxial YIG film are treated using an approach which integrates field theory with the coupled-mode approach. The MSFVW reflectivity per groove is found to be comparable to the reflectivity of magnetostatic surface waves (MSSW's) and thus is found to be

Manuscript received June 1, 1978; revised August 8, 1978. This work was supported in part by the National Science Foundation under Grant ENG-7712151, and in part by a Research Fellowship awarded to J. P. Parekh by the Research Foundation of the State University of New York.

J. P. Parekh is with the Department of Engineering, State University of New York Maritime College, Fort Schuyler, Bronx, NY 10465, and with the Department of Electrical Engineering, State University of New York at Stony Brook, Stony Brook, NY 11794.

H. S. Tuan is with the Department of Electrical Engineering, State University of New York at Stony Brook, Stony Brook, NY 11794.

significantly large considering that the volume waves are reflected by surface-localized and shallow grooves.

#### I. INTRODUCTION

A CLASS OF high-performance surface-acoustic-wave (SAW) devices such as resonators and bandpass and chirp filters which are based on the use of shallow-grooved reflector arrays has recently emerged, see for example [1]. A potential exists for the realization of similar devices operating at higher frequencies based on the use of magnetostatic waves in epitaxial YIG films. Recent experimental [2] and theoretical [3]–[5] studies have shown that magnetostatic surface waves (MSSW's) on a YIG film are reflected significantly more strongly by a groove than are SAW's by an equivalent groove on a

$\text{LiNbO}_3$  substrate. While the MSSW reflectors have potential for application to resonator and filter structures, these structures must employ normal or near-normal incidence of the MSSW at the grooves because of the limited range of angle over which MSSW propagation can exist [6], [7]. In contrast, magnetostatic forward volume waves (MSFVW's) [8]–[10] obtaining in a YIG film magnetized normal to its surface are isotropic and thus amenable for application to oblique-incidence grooved reflector configurations, e.g., ring resonators and filters, chirp filters, and contiguous filter banks. The present paper represents the first theoretical treatment of MSFVW shallow-grooved reflector gratings which employs field theory in conjunction with the theory of two-mode coupling. The approach used here parallels our previously reported studies of SAW [11] and MSSW [4] grooved reflector gratings. In parallel with these previously reported studies of SAW and MSSW grooved reflector gratings and as a first step towards a general theory for the reflection of the MSFVW incident obliquely at a grooved grating, only the normal-incidence problem is treated in this paper. It is found that the MSFVW reflectivity per groove is significantly large considering that the volume-wave reflector, viz., the grooved grating, is surface localized and shallow.

## II. THEORY

The geometry of the problem treated here is shown in Fig. 1. The grating is comprised of  $N$  identical grooves of constant cross-sectional profile in the  $y$  direction which are spaced with a period  $p$  along the  $x$  direction. Thus the total length of the grating is  $L = (N-1)p$ . The YIG film thickness is denoted  $d$ ; the groove height is denoted  $h$ ; the groove width is denoted  $2a$  corresponding to the separation between two points on a groove which are halfway down the groove. Since only the normal-incidence problem is treated in this paper, the incident MSFVW traveling in the  $+x$  direction impinges on the grating from the left. Thus all field quantities vary with the space coordinates  $x$  and  $z$  only, i.e., they are independent of  $y$ . A boundary perturbation analysis is performed which requires the grooves to be shallow; hence it is assumed that  $\epsilon = h/\lambda \ll 1$  where  $\lambda$  is the wavelength of the MSFVW. The grooves are considered to be almost rectangular so that the external saturating bias field  $H_0 \mathbf{i}_z$ , applied normal to the film, may be assumed to produce an internal field  $\mathbf{H}_i$  and saturation magnetization  $\mathbf{M}_0$  which are uniform within the film and  $z$  directed, i.e.,  $\mathbf{H}_i = H_i \mathbf{i}_z$  and  $\mathbf{M}_0 = M_0 \mathbf{i}_z$ .

The solution technique for determining the reflection characteristics of a grating of shallow grooves employing an integration of the field theory and the coupled-mode approach has previously been described in detail in the context of SAW [11] and MSSW [4] reflectors. As in the case of MSSW grooved reflectors [4], loss of power through bulk-wave generation outside of the YIG film is nonexistent simply because, in the magnetostatic limit, plane waves in the air and gadolinium-gallium-garnet

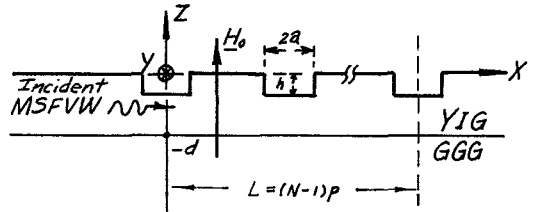


Fig. 1. Geometry of the MSFVW grooved reflector grating.

(GGG) regions are purely of the inhomogeneous variety. This absence of bulk-wave loss in the present problem simplifies the solution technique significantly over that for SAW reflectors. In the SAW reflector problem, three modes are actually coupled in the grooved-grating region, viz., the incident and reflected SAW's and the bulk waves, with the result that a two-mode coupling characterization of the problem is valid only at and in the vicinity of the array synchronous frequency where the bulk-wave loss is small and, therefore, is treated as a perturbation on the coupling of the two other modes. In the present problem there truly exist only two modes in the grooved-grating region that are coupled together, viz., the incident and reflected MSFVW's. Thus the solution is valid at all frequencies lying within the magnetostatic-volume-wave (MSVW) spectrum.

The magnetic potentials  $\phi_+^{(\text{AIR})}$ ,  $\phi_+^{(\text{YIG})}$ , and  $\phi_+^{(\text{GGG})}$  in the AIR, YIG, and GGG regions, respectively, which describe the MSFVW impinging on the grating, are solutions of the magnetostatic wave equations

$$\frac{\partial^2 \phi}{\partial x^2} + \frac{\partial^2 \phi}{\partial z^2} = 0, \quad \text{AIR and GGG regions} \quad (1)$$

and

$$\mu \frac{\partial^2 \phi}{\partial x^2} + \frac{\partial^2 \phi}{\partial z^2} = 0, \quad \text{YIG region} \quad (2)$$

satisfying appropriate boundary conditions, i.e., tangential magnetic field and normal magnetic induction are continuous across the surfaces  $z=0$  and  $z=-d$ . In (2),  $\mu = (f^2 - f_3^2)/(f^2 - f_0^2)$  is the  $xx$  or  $yy$  component of the permeability tensor characterizing the YIG medium where  $f_3 = [f_0(f_0 + f_M)]^{1/2}$  is the upper bound of the MSVW spectrum  $f_0 \leq f \leq f_3$ , or, alternatively, the lower bound of the MSSW spectrum given, for MSSW localized at an unmetallized YIG surface, by  $f_3 \leq f \leq f_0 + 0.5f_M$ . The frequencies  $f_0 = \gamma\mu_0 H_i$  and  $f_M = \gamma\mu_0 M_0$  ( $\gamma = 2.8$  MHz/G) are the gyrofrequency and magnetization frequency, respectively. It is readily shown that these potentials have the expressions

$$\phi_+^{(\text{AIR})} = \left( \frac{j2\beta}{1+j\beta} \right) A_0 \exp(-kz) \exp(-jkx), \quad z \geq 0$$

$$\begin{aligned} \phi_+^{(\text{YIG})} = A_0 \left[ \exp(-j\beta kz) - \frac{(1-j\beta)}{(1+j\beta)} \right. \\ \left. \cdot \exp(j\beta kz) \right] \exp(-jkx), \quad -d \leq z \leq 0 \end{aligned}$$

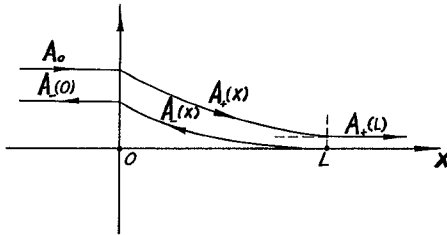


Fig. 2. Qualitative variation of the amplitudes of the incident and reflected MSFVW's within and outside the grating region.

and

$$\begin{aligned} \phi_+^{(GGG)} = & \left( \frac{j2}{1+j\beta} \right) A_0 (\sin \beta kd + \beta \cos \beta kd) \\ & \cdot \exp [k(z+d)] \exp (-jkx), \quad z \leq -d \end{aligned} \quad (3)$$

where the time-harmonic dependence  $\exp(j2\pi ft)$  has been suppressed, and the wave number  $k = 2\pi/\lambda$  of the incident (or reflected) wave satisfies the MSFVW dispersion relation

$$|k| = \frac{1}{\beta d} \tan^{-1} \left( -\frac{2\beta}{1-\beta^2} \right) \quad (4)$$

with

$$\beta = (-\mu)^{1/2}.$$

As the incident MSFVW progresses through the grating, its amplitude  $A_+(x)$  decreases monotonically from the known value  $A_+(0) = A_0$  at the start  $x=0$  of the grating to some value  $A_+(L)$  at the end  $x=L$  of the grating. Beyond the grating, the amplitude remains constant at  $A_+(L)$  corresponding to the transmitted wave. Similarly, the amplitude  $A_-(x)$  of the reflected MSFVW shows a monotonic increase from  $A_-(L) = 0$  at the end of the grating to some value  $A_-(0)$  at the start of the grating. For  $x < 0$ ,  $A_-(x)$  remains constant at  $A_-(0)$  corresponding to the amplitude of the MSFVW reflected by the grating. For  $x > L$ ,  $A_-(x)$  must clearly be zero for all  $x$  since a reflected MSFVW does not exist beyond the grating. The qualitative features of the  $x$  variation of  $A_+(x)$  and  $A_-(x)$  are shown in Fig. 2.

The assumption of shallow grooves leads to the result that energy loss due to the reflection from a single groove is [14], [15] of the order  $\epsilon^2$ . This energy loss occurs over the length of a groove which is of the order of  $\lambda$ . Therefore, in the grating region, the potential functions describing the incident and reflected MSFVW's within and outside of the grating region are

$$\begin{aligned} \phi_{\pm}^{(AIR)} = & \left( \frac{j2\beta}{1+j\beta} \right) A_{\pm}(x) \exp(-kz) \exp(\mp jkx), \quad z \geq 0 \\ \phi_{\pm}^{(YIG)} = & A_{\pm}(x) \left[ \exp(-j\beta kz) - \frac{(1-j\beta)}{(1+j\beta)} \exp(j\beta kz) \right] \\ & \cdot \exp(\mp jkx), \quad -d \leq z \leq 0 \\ \phi_{\pm}^{(GGG)} = & \left( \frac{j2}{1+j\beta} \right) A_{\pm}(x) (\sin \beta kd + \beta \cos \beta kd) \\ & \cdot \exp[k(z+d)] \exp(\mp jkx), \quad z \leq -d \end{aligned} \quad (5)$$

where the nonuniform amplitude functions  $A_{\pm}(x)$  do not vary appreciably over a distance  $\lambda$ . These amplitude functions are obtained from the two-mode coupling analysis [12], [13] to be

$$A_+(x) = A_0 \cosh \left[ KL \left( 1 - \frac{x}{L} \right) \right] \operatorname{sech} KL \quad (6)$$

and

$$A_-(x) = A_-(0) \sinh \left[ KL \left( 1 - \frac{x}{L} \right) \right] \operatorname{cosech} KL \quad (7)$$

where  $K$  is an unknown phenomenological coupling constant and  $A_-(0)$  is the unknown amplitude of the reflected wave. From (6) and (7), the MSFVW amplitude reflection coefficient of the grating is  $R(0) = A_-(0)/A_0$ . By imposing the requirement of energy conservation on the grating, it is readily shown that  $|A_-(0)| = |A_0| \tanh KL$ . Thus the coupled mode theory yields

$$|R(0)| = \tanh KL. \quad (8)$$

Since in (8)  $K$  is an unknown, a second relation connecting  $|R(0)|$  and  $K$  must be found in order to determine  $|R(0)|$ . This second relation is obtained from field theory by employing a boundary perturbation approach described in detail elsewhere in the context of the SAW scattering from a single shallow groove [14] or from a shallow-grooved grating [11]. In the present work, only a brief description of the perturbation theory will be given.

Since the incident MSFVW specified in (5) cannot by itself satisfy the boundary conditions at the grooved YIG surface, the existence of scattered fields must be postulated. Because of the weak-scatterer nature of the shallow grooves, the total fields may be expressed as the power-series expansion

$$\begin{aligned} \phi^{(AIR)} = & \phi_+^{(AIR)} + \sum_{m=1}^{\infty} \epsilon^m \phi_m^{(AIR)} \\ \phi^{(YIG)} = & \phi_+^{(YIG)} + \sum_{m=1}^{\infty} \epsilon^m \phi_m^{(YIG)} \\ \phi^{(GGG)} = & \phi_+^{(GGG)} + \sum_{m=1}^{\infty} \epsilon^m \phi_m^{(GGG)} \end{aligned} \quad (9)$$

in the small parameter  $\epsilon$ . Since  $\epsilon$  is just a parameter and the total fields  $\phi^{(AIR)}$ ,  $\phi^{(YIG)}$ , and  $\phi^{(GGG)}$  satisfy the magnetostatic wave equations (1) and (2), it follows that  $\phi_m^{(AIR)}$ ,  $\phi_m^{(YIG)}$ , and  $\phi_m^{(GGG)}$  also satisfy these equations for each value of  $m$ . The boundary conditions require the tangential magnetic field and the normal magnetic induction to be continuous across the top (grooved) and bottom (planar) surfaces of the YIG film.

In the boundary perturbation technique, the tangential magnetic field and normal magnetic induction are expanded in a Taylor series in  $z$  about  $z=0$ , and the coefficient function for each power term of  $\epsilon$  is required to vanish because of the nonmixing property of the different power terms of  $\epsilon$ . This procedure is equivalent to replacing the original problem with an equivalent problem of finding the potentials  $\phi_m^{(AIR)}$ ,  $\phi_m^{(YIG)}$ , and  $\phi_m^{(GGG)}$  (for each  $m$ ) in an *ungrooved* YIG film geometry which are excited

by a magnetic surface charge [16] distribution  $\eta(x, 0)$  and an electric surface current distribution  $J_y(x, 0)$  located on the ungrooved surface  $z=0$  within the region  $0 \leq x \leq L$ . For the first-order scattered fields, these *equivalent* or *induced* surface sources on an ungrooved YIG film surface within the region occupied by the grating in a grooved geometry are

$$\begin{aligned} \eta(x, 0) = \mu_0 \lambda f(x) \left[ -\frac{\partial^2 \phi_+^{(\text{AIR})}}{\partial z^2}(x, 0) + \frac{\partial^2 \phi_+^{(\text{YIG})}}{\partial z^2}(x, 0) \right] \\ + \mu_0 \lambda \frac{df(x)}{dx} \left[ \frac{\partial \phi_+^{(\text{AIR})}}{\partial x}(x, 0) - \mu \frac{\partial \phi_+^{(\text{YIG})}}{\partial x}(x, 0) \right] \quad (10) \end{aligned}$$

and

$$\begin{aligned} J_y(x, 0) = \mu_0 \lambda f(x) \left[ \frac{\partial^2 \phi_+^{(\text{AIR})}}{\partial x \partial z}(x, 0) - \frac{\partial^2 \phi_+^{(\text{YIG})}}{\partial x \partial z}(x, 0) \right] \\ + \mu_0 \lambda \frac{df(x)}{dx} \left[ \frac{\partial \phi_+^{(\text{AIR})}}{\partial z}(x, 0) - \frac{\partial \phi_+^{(\text{YIG})}}{\partial z}(x, 0) \right] \quad (11) \end{aligned}$$

where  $\mu_0$  is the permeability of free space and  $f(x)$  is the function defining the profile of the grooved grating. Since  $f(x)$  and  $df(x)/dx$  are zero outside of the grating region, the induced sources, as expected, are seen from (10) and (11) to depend only on the incident MSFVW within the grating region and the profile of the grating.

Using the standard Fourier transform technique, the foregoing equivalent source problem in an ungrooved YIG film geometry readily yields integral expressions for the first-order scattered-field potentials. The residue contributions to these integrals at the pole corresponding to the reflected wave yields the expressions for the potentials  $\phi_+^{(\text{AIR})}$ ,  $\phi_+^{(\text{YIG})}$ , and  $\phi_-^{(\text{GGG})}$ . The residue calculation is greatly simplified by the assumption that the grooves are individually weak scatterers, i.e., the amplitude function  $A_+(x)$  varies very slowly with  $x$ . It is found that the resulting approximate expression for the MSFVW amplitude reflection coefficient of the grating may be written as

$$R(0) = -j(h/\lambda) \zeta k H(-k) \quad (12)$$

where  $\zeta$  is an array factor and  $H(-k) = \lim_{\xi \rightarrow -k} H(\xi)$ , with  $H(\xi)$  being the Fourier transform of the function  $f_1(x) \exp(-jkx)$  where  $f_1(x)$  is a function defining the profile of a single groove centered at the origin. For grooves that are almost rectangular, the expression for  $H(-k)$  is [14]

$$H(-k) \approx -k^{-1} \sin 2ka. \quad (13)$$

The array factor  $\zeta$  has the expression

$$\zeta = \frac{1}{2 \cosh KL} \left\{ \frac{(1 - g^N e^{-N\nu})}{(1 - g e^{-\nu})} e^{\kappa L} + \frac{(1 - g^N e^{N\nu})}{(1 - g e^\nu)} e^{-\kappa L} \right\} \quad (14)$$

where  $\nu = Kp$  and  $g = \exp(-j2kp)$ .

Equation (12) reduces to the expression for the first-order MSFVW reflection coefficient for a single groove

[15] by making the array factor  $\zeta$  unity. For a grating, (8) and (12) provide two equations in two unknowns, viz.,  $|R(0)|$  and  $K$ , which need to be solved simultaneously using an iterative procedure. Once these unknowns are found, the complex reflection coefficient  $R(0)$  is obtained by substituting the value of  $K$  into (12). The reflection coefficient  $R(0)$  depends on the groove width  $2a$  through the function  $H(-k)$  in (13) and on the groove periodicity  $p$  through the function  $g$  in (14). The optimum values of  $2a$  and  $p$  which maximize  $|R(0)|$  are  $2a = \lambda/4$  and  $p = \lambda/2$ . In order to design a MSFVW reflector with known YIG film parameters and for operation at a prescribed frequency and bias field, one needs to solve (4) for  $\lambda$  pertinent to these parameters and then to use the foregoing optimum values of groove width and periodicity.

### III. NUMERICAL RESULTS AND DISCUSSION

The theoretical results obtained in Section II apply to any of the even or odd MSFVW modes supported by the YIG film. The dispersion curve for any particular mode corresponds [8], [10] to a monotonic increase in  $k$  and  $dk/df$  with a frequency over the MSVW spectrum, with a resonance ( $k \rightarrow \infty$ ) occurring at the upper bound of the spectrum. As the mode number is increased at a fixed frequency, the dispersion curve shifts in the direction of increasing  $k$ . The effect of this increase in  $k$  with mode number at a given frequency is readily interpreted for the case of the MSFVW reflection by a single groove as explained below.

#### A. MSFVW Reflectivity of a Single Groove

From (12) and (13) it is seen that the frequency variation of  $|R(0)|/(h/\lambda)$  exhibits maxima at frequencies corresponding to  $2ka = (2n+1)\pi/2$ ,  $n=0, 1, 2, \dots$ , and zeroes at frequencies corresponding to  $2ka = m\pi$ ,  $m=1, 2, 3, \dots$ . The reflection coefficient at all of these maxima has the same value  $|R(0)|_{\max} = h/\lambda$ . For  $h/\lambda = 0.015$ , this yields a value  $|R|_{\max} = 1.5$  percent which is approximately 150 percent of the SAW amplitude reflection coefficient  $R = 0.9$  percent obtaining for a groove of the same geometry and normalized depth on a  $y$ -cut  $z$ -propagating  $\text{LiNbO}_3$  [11]. The value of  $|R(0)|_{\max}$  obtained here is somewhat comparable to the peak value of  $|R(0)|_{\max}$  obtaining for the MSSW reflectivity of a single groove of the same geometry and normalized depth on a YIG film [5]. In light of the fact that in the present work it is volume waves that are reflected by grooves that are surface localized as well as shallow, it is concluded that the MSFVW reflectivity of a groove is significantly large.

The effect on  $R(0)$  of increasing the YIG film thickness  $d$  is readily interpreted from (4), (12), and (13). Equation (4) shows that at a given frequency the MSFVW wavelength  $\lambda$  is directly proportional to  $d$ . Thus, from (12) and (13), for a fixed groove depth  $h$ ,  $|R(0)|_{\max}$  is inversely proportional to  $d$ . It is evident that  $|R(0)|_{\max}$  remains independent of  $d$  if  $h$  is changed in direct proportion to  $d$ .

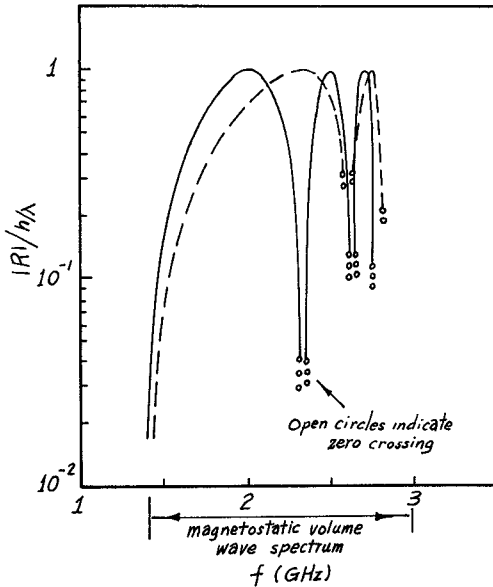


Fig. 3. Frequency variation of the MSFVW reflection coefficient for a single shallow groove, with  $\mu_0 H_i = 500$  G,  $\mu_0 M_0 = 1750$  G,  $d = 10$   $\mu\text{m}$ ,  $2a = 10$   $\mu\text{m}$  (dashed curve), and  $2a = 20$   $\mu\text{m}$  (solid curve).

In Fig. 3, computed frequency variation of  $|R(0)|$  is presented for the lowest MSFVW mode. Also, all other computations presented in this paper are for the lowest MSFVW mode, with the values of the internal bias field  $\mu_0 H_i$ , saturation magnetization  $\mu_0 M_0$ , and YIG film thickness  $d$  being chosen to be 500 G, 1750 G, and 10  $\mu\text{m}$ , respectively. The dashed curve in Fig. 3 corresponds to groove width  $2a = 10$   $\mu\text{m}$  and the solid curve to groove width  $2a = 20$   $\mu\text{m}$ . Only the lowest two peaks are shown on the dashed curve and only the lowest three peaks on the solid curve since the increasingly smaller frequency spacing of the higher peaks makes them difficult to show on the frequency scale used. The monotonic and rapid decrease in the frequency spacing of the peaks is consistent with the MSFVW dispersion characteristics, viz., the MSFVW dispersion curve for a given  $d$  and a given mode corresponds to a monotonic increase in  $k$  and  $dk/df$  with frequency. The effect of changing the mode number from one value to a higher value is apparent, i.e., the frequencies corresponding to  $|R(0)|_{\max}$  are lowered. Thus the effect of increasing the mode number for a given groove width is qualitatively equivalent to increasing the groove width for a fixed mode number. This behavior is implied by the  $\sin 2ka$  factor in (13).

#### B. MSFVW Reflectivity of a Grooved Grating

In Fig. 4, the variation with  $N$  of the grating reflectivity is presented for a fixed frequency  $f = 2.02$  GHz, groove width  $2a = 20$   $\mu\text{m}$ , grating period  $p = 40$   $\mu\text{m}$ , and five values of the groove height, i.e.,  $h/\lambda = 0.005, 0.010, 0.015, 0.020$ , and  $0.025$ . The curves in Fig. 4 correspond to the maximum reflectivity point on the *lowest* peak of the solid curve in Fig. 3, which occurs at  $f = 2.02$  GHz and  $\lambda = 80$   $\mu\text{m}$ . In order to highlight the small deviation from 1 of  $|R(0)|$  for large values of  $N$ , a plot of  $1 - |R(0)|$  versus  $N$  is

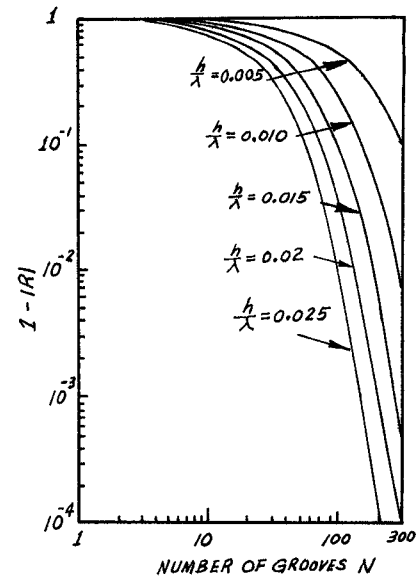


Fig. 4. Variation with  $N$  of  $1 - |R(0)|$  for a MSFVW grooved grating, with  $f = 2.02$  GHz,  $2a = 20$   $\mu\text{m}$ ,  $p = 40$   $\mu\text{m}$ ,  $\mu_0 H_i = 50$  G,  $\mu_0 M_0 = 1750$  G, and  $d = 10$   $\mu\text{m}$ . The normalized groove depth  $h/\lambda$  is taken as a parameter.

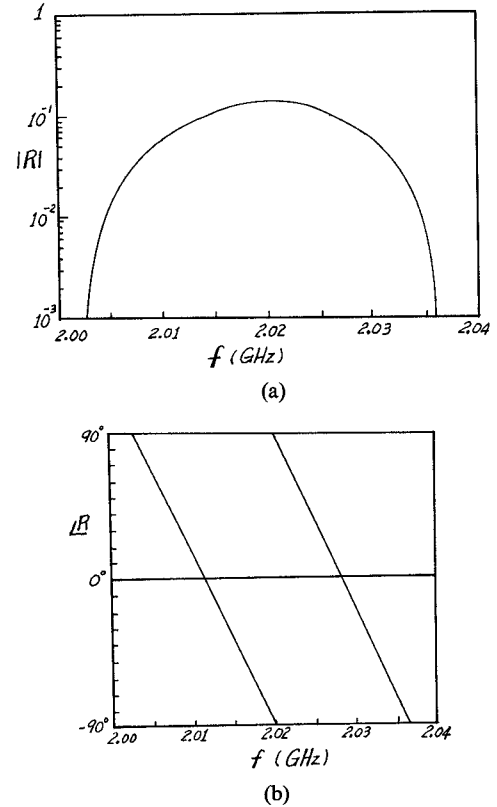


Fig. 5. Frequency variation of the (a) amplitude and (b) phase of  $R(0)$  for a grooved grating, with  $N = 25$ ,  $2a = 20$   $\mu\text{m}$ ,  $p = 40$   $\mu\text{m}$ ,  $\mu_0 H_i = 500$  G,  $\mu_0 M_0 = 1750$  G,  $d = 10$   $\mu\text{m}$ , and  $h/\lambda = 0.005$ .

presented, and a logarithmic scale is used. As  $h/\lambda$  is increased for a given  $N$ ,  $|R(0)|$  is seen to go up in agreement with expectation.

In Fig. 5, the effect of moving off the synchronous frequency of a grating is shown for a grating comprised of  $N = 25$  grooves and of parameters  $2a = 20$   $\mu\text{m}$ ,  $p = 40$   $\mu\text{m}$ ,

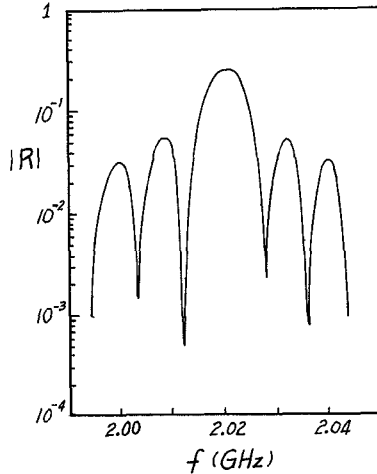


Fig. 6. Frequency variation of  $|R(0)|$  for a grooved grating with  $N=50$ ,  $2a=20 \mu\text{m}$ ,  $p=40 \mu\text{m}$ ,  $\mu_0 H_i=500 \text{ G}$ ,  $\mu_0 M_0=1750 \text{ G}$ ,  $d=10 \mu\text{m}$ , and  $h/\lambda=0.005$ .

and  $h/\lambda=0.005$ , i.e., the frequency variation of the magnitude and phase of  $R(0)$  is presented in the vicinity of the synchronous frequency  $f=2.02 \text{ GHz}$ . Only a small frequency interval around the synchronous frequency is taken in Fig. 5 in order to indicate details of variation of the magnitude and phase of  $R(0)$ . As expected, the reflection coefficient  $R(0)$  undergoes a phase change of  $180^\circ$  as the frequency is increased through the synchronous frequency. A conspicuous feature of Fig. 5(b) is the linear variation of the phase with frequency. Finally, Fig. 6 illustrates the reduction in bandwidth of the principal lobe in Fig. 5(a) with an increase in the number of grooves in the grating. The curve in Fig. 6 was computed for  $N=50$ , with all the other parameters being the same as in Fig. 5. The existence of subsidiary lobes on either side of the principal lobe is evident in Fig. 6.

#### IV. CONCLUSION

The MSFVW reflection characteristics of a shallow-grooved grating etched on top of a YIG film are treated for the case of normal incidence. The MSFVW reflectivity is found to be comparable to the reflectivity of the MSSW

in a similar geometry and thus to be significantly large considering that the volume waves are scattered by grooves that are shallow and surface localized. The absence of the MSVW generation outside of the YIG film region suggests that by deepening the grooves so that they are no longer shallow, the MSFVW reflectivity of a grating might be further enhanced, thereby reducing the number of grooves needed to produce a prescribed reflectivity.

#### REFERENCES

- [1] *Proc. 1977 IEEE Ultrasonics Symp.* New York: IEEE, 1977.
- [2] C. G. Sykes, J. D. Adam, and J. H. Collins, "Magnetostatic wave propagation in a periodic structure," *Appl. Phys. Lett.*, vol. 29, pp. 388-391, Sept. 1976.
- [3] J. P. Parekh and H. S. Tuan, "Magnetostatic surface wave reflectivity of a shallow groove on a YIG film," *Appl. Phys. Lett.*, vol. 30, pp. 667-669, June 1977.
- [4] —, "Theory for a magnetostatic surface wave grooved reflector grating," *IEEE Trans. Magn.*, vol. MAG-13, pp. 1246-1248, Sept. 1977.
- [5] —, "Reflection of magnetostatic surface wave at a shallow groove on a YIG film," *Appl. Phys. Lett.*, vol. 31, pp. 709-712, Nov. 1977.
- [6] R. W. Damon and J. R. Eshbach, "Magnetostatic modes of a ferromagnet slab," *J. Phys. Chem. Solids*, vol. 19, pp. 308-320, 1961.
- [7] J. P. Parekh, "Magnetostatic surface waves on a partially metallized YIG plate," *Proc. IEEE*, vol. 61, pp. 1371-1373, Sept. 1973.
- [8] R. W. Damon and H. van de Vaart, "Propagation of magnetostatic spin waves at microwave frequencies in a normally-magnetized disc," *J. Appl. Phys.*, vol. 36, pp. 3453-3459, Nov. 1965.
- [9] Z. M. Bardai, J. D. Adam, J. H. Collins, and J. P. Parekh, "Delay lines based on magnetostatic volume waves in epitaxial YIG," in *AIP Conf. Proc. no. 34*, (1976 Joint MMM-Intermag. Conf.), pp. 268-270.
- [10] T. Yukawa and J. Ikenoue, "Effects of metal on dispersion relations of magnetostatic volume waves," *J. Appl. Phys.*, vol. 49, pp. 376-382, Jan. 1978.
- [11] H. S. Tuan and J. P. Parekh, "Theory for SAW grooved reflector arrays," *IEEE Trans. Sonics Ultrason.*, vol. SU-24, pp. 384-392, Nov. 1977.
- [12] M. Kogelnik and C. V. Shank, "Coupled-wave theory of distributed feedback lasers," *J. Appl. Phys.*, vol. 43, pp. 2327-2335, 1972.
- [13] A. Yariv, "Coupled-mode theory for guided-wave optics," *IEEE J. Quantum Electron.*, vol. QE-9, pp. 919-933, Sept. 1973.
- [14] J. P. Parekh and H. S. Tuan, "Reflection and bulk-wave conversion of Rayleigh wave at a single shallow groove," *J. Appl. Phys.*, vol. 48, pp. 994-1003, Mar. 1977.
- [15] —, "Magnetostatic forward volume wave reflection by a shallow groove on a YIG film," *Appl. Phys. Lett.*, vol. 33, pp. 267-269, Aug. 1978.
- [16] C. H. Pappas, *Theory of electromagnetic wave propagation*. New York: McGraw-Hill, 1965.